Optics Letters

Cascaded downconversion interface to convert single-photon-level signals at 650 nm to the telecom band

VAHID ESFANDYARPOUR,* CARSTEN LANGROCK, AND MARTIN FEJER

E. L. Ginzton Laboratory, Stanford University, 348 Via Pueblo Mall, Stanford, California 94305, USA
**Corresponding author: vahid@alumni.stanford.edu*

Received 28 August 2018; revised 13 October 2018; accepted 15 October 2018; posted 16 October 2018 (Doc. ID 342897); published 14 November 2018

We present a device designed for two-step downconversion of single-photon-level signals at 650 nm to the 1.5-μm band with low excess noise and low required pump power as a quantum interface between matter-qubit-based nodes and low-loss photonic channels for quantum communication networks. The required pump power for this interface is around 60% of that for a comparable conventional single-pass device, which reduces the demand on the pump laser and yields a corresponding reduction in dark counts due to inelastic pump scattering. The single-photon-level signal at 649.7 nm is downconverted to the telecom band using a fiber-coupled reverse proton exchange periodically poled lithium niobate waveguide and a 2.19-μm pump laser. By testing the device in the linear regime with a classical input, we achieved 99% depletion efficiency for each stage, corresponding to an internal quantum efficiency of 63% at the optimum pump power for the complete cascaded process.

https://doi.org/10.1364/OL.43.005655

The need for interfaces between quantum nodes and low-loss quantum channels in long-distance quantum communication networks [1,2] motivates the development of quantum frequency conversion (QFC) devices, in which a qubit's carrier frequency is translated while its quantum state is maintained [3–5]. Frequency conversion in $\chi^{(2)}$ media by either sum- or difference-frequency generation (DFG) can interchange quantum states of light between two frequencies ω_1 and ω_2 via interaction with a strong optical pump at ω_p, with $\omega_1 \pm \omega_p = \omega_2$ [3].

Quantum dots have been studied as potential quantum network nodes [6,7], and frequency conversion of visible and near-infrared photons from trapped ions, color centers, and quantum dots has been demonstrated [8,9]. However, generation of noise photons in the conversion process limited the utility of the QFC technique for quantum networks. Implementing such an interface between matter qubits (which typically have optical transitions in the visible or near-infrared spectral range) and low-loss photonic quantum channels (at the 1.3- or 1.5-μm low-loss bands in silica optical fibers) is a primary challenge toward developing long-distance hybrid quantum networks. In this work, we describe a novel cascaded QFC scheme whereby visible photons at the wavelength 649.7 nm (the wavelength emitted by $^{138}Ba^{+}$ ions) are downconverted to the 1.5-μm band with low dark counts and high quantum efficiency, and demonstrate it with a classical input in the linear regime.

QFC interfaces have been demonstrated in both bulk and waveguide configurations [1,5,10–18]. A key issue in these devices is minimizing the generation of noise photons in the signal band by inelastic scattering of the pump. Several QFC experiments were targeted to the 1.3-μm window [8,19,20], for which low-noise conversion is more easily attained than at 1.5 μm. However, the lower losses in silica fibers at 1.5 μm suggest that a solution reducing the inelastic scattering for conversion to this wavelength range would be advantageous. Operation at 1.5-μm would almost double the transmission distance compared to 1.3 μm due to lower losses in silica fibers.

One main concern about a 1.5-μm interface is the large dark count rate due to spontaneous scattering processes of the strong classical pump [11,14]. To address this problem, it is necessary to choose a pump frequency ω_p substantially lower than that of any other photons involved in the conversion process [11,14]. It has recently been shown that long-wavelength pumping dramatically reduces the dark-count rate [1,11,21,22]. This requirement limits the wavelength-translation range which can be achieved in a single conversion step [23], leading to the development of integrated devices based on two cascaded parametric conversion processes [23,24]. For the translation of photons from 650 nm to 1.59 μm described here, a 2.19-μm pump is used, with a first conversion step to an intermediate wavelength of 923 nm and a second step converting the 923-nm photons to the telecom band to satisfy the condition for low-noise operation.

In this approach, which is diagrammed schematically in Fig. 1, by using sequential quasi-phase-matching (QPM) gratings, a two-step process can be achieved: in a first DFG process (DFG-A), a long-wavelength pump at ω_p is differenced with

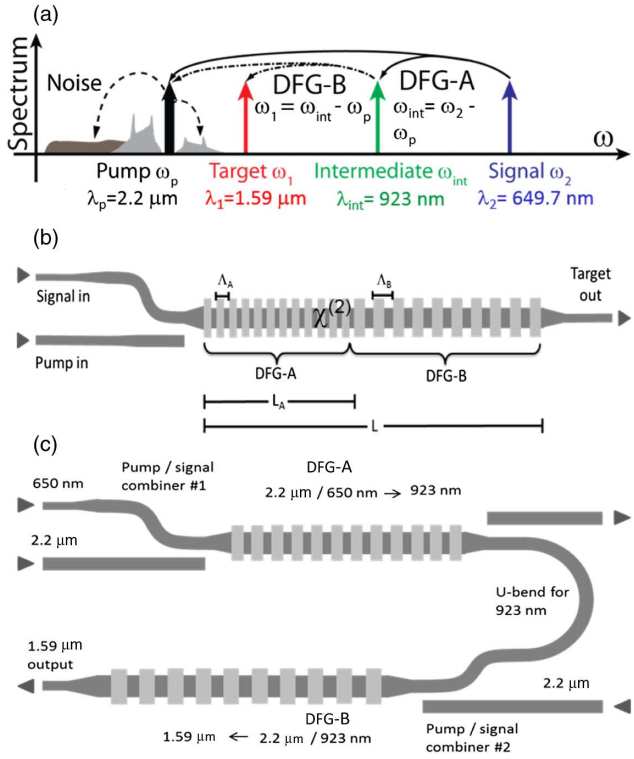

Fig. 1. (a) Schematic of the frequencies involved in a two-step cascaded process, (b) conventional PPLN waveguide design for the two-stage downconversion process, and (c) schematic design for a double-pass converter.

the input signal at ω_1 to produce radiation at $\omega_{\text{int}} = \omega_2 - \omega_p$. A second DFG process (DFG-B) differences the pump with the photons at ω_{int} to produce the target radiation at $\omega_1 = \omega_{\text{int}} - \omega_p = \omega_2 - 2\omega_p$. For an input signal at $\lambda_2 = 649.7$ nm, a pump wavelength at $\lambda_p = 2.19$ μm was used to satisfy the constraint for low noise operation, resulting in $\lambda_{\text{int}} = 923.4$ nm and $\lambda_1 = 1.59$ μm.

In conventional cascaded frequency conversion devices, a single waveguide with sequential QPM gratings is used for a two-step process, as is shown in Fig. 1(b). The length of this type of device is limited by the wafer size. By implementing a 180° turn (U-bend) and carrying out one of the two DFG process in each arm, which doubles the wafer-size-limited effective conversion length, it is possible to expand the device length beyond the wafer diameter without incurring losses due to in- and outcoupling multiple waveguides, resulting in a reduction of the required pump power for complete conversion of the input photons, Fig. 1(c). With a properly designed U-bend that strongly attenuates the noise photons generated in the first arm, together with the reduction in the required pump power, a proportional reduction in the output noise photons results. The possibility of controlling the pump power for each process separately, to optimize each conversion process independently, is another advantage which is not practical in a single-pass device.

In this Letter, we describe aspects of the theory and design constraints of making a U-bend structure for cascaded downconversion. We designed and fabricated the double-pass converter shown in Fig. 1(c), and with such a device, we achieved more than 99% depletion efficiency for each process, corresponding to an overall internal conversion efficiency of 63%, limited by waveguide propagation losses at the optimum pump power for the complete cascaded process. The required pump power is around 60% of the required power for the conventional straight and single-pass waveguides with sequential QPM gratings.

The cascaded downconversion process was carried out in a periodically poled lithium niobate (PPLN) waveguide fabricated using the reverse-proton-exchange technique [1,10,11]. The waveguide chip had a total length of 5.65 cm and had a periodically poled grating of 3.81-cm length with period $\Lambda_{G-A} = 12.29$ μm for the first process and 4.5-cm length with periodicity $\Lambda_{G-B} = 22.83$ μm for the second process. The waveguide incorporated mode filters and adiabatic tapers to spatially mode match the two input waveguides of the device to optical fibers, PM-650 fiber for the signal at 650 nm and PM-1550 for the pump at 2.2 μm. The main waveguide in each arm was optimized for mixing efficiency, which leads to their being multimode for 1.5 μm and 650 nm. With the use of mode filters, adiabatic tapers, and S-bend in the input section, only a single mode is launched at the inputs, and phase-matching constraints lead to only a single mode being generated in the mixing processes, which was confirmed by having single-peak sinc^2 phase-matching curves.

The schematic of the experiment is shown in Fig. 2. Pump light at 2.19 μm was generated with a tunable Cr^{2+}:ZnSe laser (IPG, model SFTLCRZNSES2200-2000). For the input, we used a classical signal in the linear regime at 649.7 nm from a CW tunable external-cavity diode laser. The purpose of using a combination of a polarizer and a half-wave plate in each arm is to control the pump power for each process separately. The pump and signal were combined into the interaction region containing the QPM grating for the first process using an integrated wavelength-division multiplexer (WDM) coupler [25] based on a directional coupler in which the pump radiation evanescently couples from one waveguide of the coupler to the other, while the signal (due to its shorter wavelength and smaller mode size) does not couple significantly.

Following the interaction region for the first process, a U-bend was used to transmit the generated radiation at λ_{int} to the second arm as the input signal for the second process. Another WDM coupler was used to combine the pump and

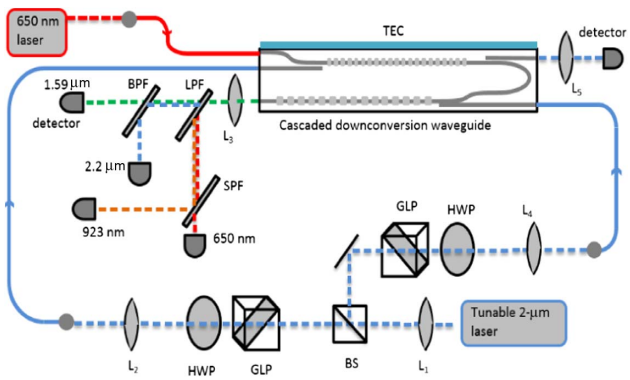

Fig. 2. Experimental setup for the cascaded DFG device. Abbreviations: L, lens; BS, beamsplitter; GLP, Glan-laser polarizer; HWP, half-wave plate; BPF, bandpass filter; LPF, long-pass filter; SPF, short-pass filter; TEC: thermo-electric cooling.

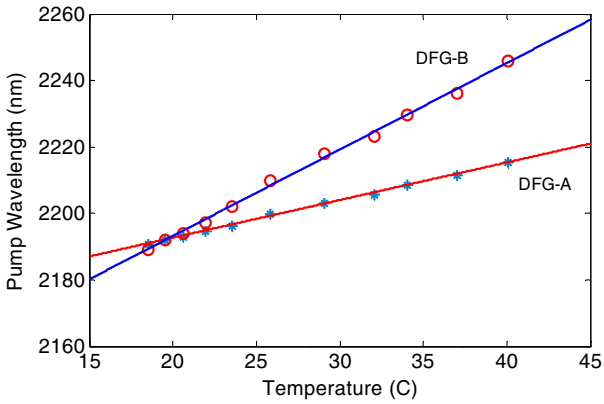

Fig. 3. Phase-matching behavior of a U-bend device. To achieve efficient two-step conversion, both processes must be phase-matched at the same temperature and pump wavelength.

intermediate frequencies into the interaction region for the second process. It was experimentally confirmed that photons in the telecom band are attenuated by more than 50 dB through the U-bend, correspondingly attenuating the noise photons in that spectral region from the first DFG stage. As the radiation loss is higher for longer wavelengths, the pump-wavelength attenuation is also more than 50 dB. We found experimentally that by choosing the U-bend radius between 2.5 and 3 mm, the radiation loss at the intermediate wavelength, $\lambda_{\text{int}} = 923$ nm, due to the 180° U-bend is only 0.13 dB, which is less than 7% of the total propagation loss of the waveguides. To measure the radiation loss through the U-bend, we fabricated straight waveguides with similar designs next to the U-bends on the same chip and measured the attenuation with the Fabry–Perot method, which is 0.15 dB/cm for 920 nm [26]. The difference between losses in straight and U-bend devices is the radiation loss due to the U-bend and is 0.13 dB for 920 nm. Wider waveguides showed unmeasurably small losses, but they are multimoded.

We first characterized the conversion efficiency of each process versus signal wavelength and temperature. To achieve efficient conversion, both DFG processes must simultaneously be tuned to their QPM peaks. DFG-A and DFG-B QPM peaks tune at a slightly different rate versus temperature, which results in a point where both processes are at their QPM peaks at the same temperature and pump wavelength. Figure 3 shows the experimental results for a pump wavelength at $\lambda_p = 2192$ nm, with which QPM for both DFG processes was observed for $\lambda_2 = 649.7$ nm and $T = 19.6$°C.

We next measured the conversion efficiency of a classical input signal in the linear regime at $\lambda_2 = 649.7$ nm. Figure 4 shows the depletion efficiencies for each process separately, namely the conversion process from 649.7 to 923 nm in the first arm and from 923 nm to telecom band in the second arm. Depletion efficiency is defined as the ratio of the input signal which is converted to the target wavelength to the total input signal. To measure depletion efficiency, we measured the ratio of the output signal power with and without the presence of the pump. As can be seen in Fig. 4, more than 99% depletion efficiency is reached for both processes; the error bars are smaller than the triangle size in the plots. A benefit of using a U-bend device is that the pump power can be optimized separately for each waveguide and each process can be measured separately. As depletion efficiencies for both processes are more than 99%, the (internal) conversion efficiency for the cascaded process is only limited by the propagation loss and the 7% excess loss in the U-bend section. There was inadequate pump power to drive both processes to complete conversion at the same time, but cascading the efficiencies measured individually for the two processes leads to a predicted efficiency of 63%, limited by the waveguide propagation losses of approximately 0.15 dB/cm for 650 and 923 nm wavelengths, and 0.2 dB/cm for the telecom wavelength region. The highest measured external conversion efficiency, limited by the available pump power, while running both processes together, was 36%, corresponding to a 47.5% internal conversion efficiency, with coupling efficiencies for 650 and 1590 nm of 90% and 85%, respectively. The measured cascaded efficiency matches the predicted cascaded efficiency by measuring the conversion efficiency for each process and loss separately. Given the 50-dB extinction of 1.5-μm light in the U-bend, the dominant noise at the output is due to anti-Stokes Raman scattering of the pump in the second waveguide. At the time of this experiment

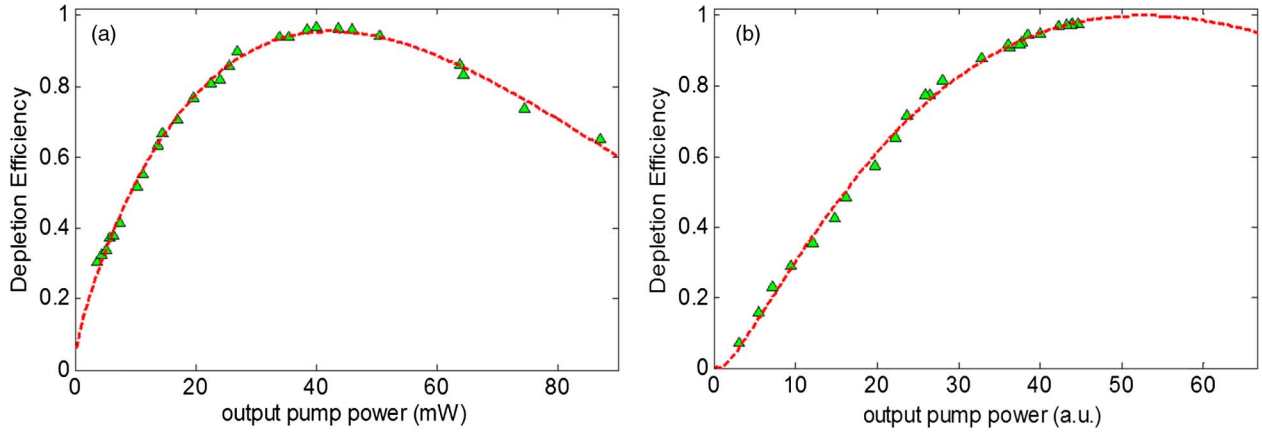

Fig. 4. Measured depletion efficiencies versus pump power at 2.192 μm (triangles) and fits to the conversion efficiency equation: (a) Depletion efficiency for the first process, (b) depletion efficiency for the second process. The output pump power for the second process is not calibrated due to unknown losses for the pump wavelength in the tapering and mode-matching sections at the output of the device. The maximum conversion efficiency in the graph corresponds to a launched pump power of 480 mW, assuming an input coupling efficiency of 80%.

we did not have access to a 1.5-μm photon counter capable of resolving the dark count rate of the converter. By extrapolating the model for anti-Stokes Raman scattering noise from [11], we calculated a dark-count rate of 1.5 count/s/GHz. We previously measured the dark-count rate on a similar single-photon downconversion device with the same pump wavelength and waveguide length and found 1.7 ± 0.3 counts/s/GHz, consistent with the predictions of the same model for the anti-Stokes Raman scattering rate [1].

To conclude, we discussed considerations in using cascaded frequency mixers for low-noise QFC between two widely disparate frequencies, such as long-wavelength-pumped downconversion of visible single photons from a diamond nitrogen-vacancy center or trapped ion to 1550 nm. The main application of the U-bend structure that we have shown in this work is the low-power, low-noise frequency conversion of visible/near-infrared wavelengths to the telecom band, which represents a critical step toward low-power, low-noise QFC for long-distance quantum communication networks. We have demonstrated a novel integrated architecture for low-noise cascaded frequency conversion, which requires lower pump power compared to conventional cascaded designs. For conversion from 649.7 to 1595 nm, with this U-bend structure we obtained depletion efficiencies of more than 99% in each arm, corresponding to an internal cascaded conversion efficiency limited by propagation losses to 63%. The required pump power for the U-bend design is around 60% of that for a comparable single-pass device, which reduces the demand on the pump laser and yields a corresponding reduction in dark counts due to inelastic pump scattering. Further reducing the pump power is possible by use of the same pump in both arms, with the price of tighter fabrication tolerances and approximate doubling of the noise. The dark count rate, which is set by anti-Stokes Raman scattering of the pump, is estimated to be less than 2 cps/GHz.

Funding. Defense Advanced Research Projects Agency (DARPA) (1160784, 1177474); The QUINESS Program.

Acknowledgment. We thank Alireza Marandi and Bob Byer's group at Stanford University for the use of their equipment.

REFERENCES

1. J. S. Pelc, L. Yu, K. De Greve, P. L. McMahon, C. M. Natarajan, V. Esfandyarpour, S. Majer, C. Schneider, M. Kamp, S. Hofling, R. H. Hadfield, A. Forchel, Y. Yamamoto, and M. M. Fejer, Opt. Express **20**, 27510 (2012).
2. H. J. Kimble, Nature **453**, 1023 (2008).
3. P. Kumar, Opt. Lett. **15**, 1476 (1990).
4. S. Tanzilli, W. Tittel, M. Halder, O. Alibart, P. Baldi, N. Gisin, and H. Zbinden, Nature **437**, 116 (2005).
5. R. Ikuta, Y. Kusaka, T. Kitano, H. Kato, T. Yamamoto, M. Koashi, and N. Imoto, Nat. Commun. **2**, 537 (2011).
6. D. Press, T. D. Ladd, B. Zhang, and Y. Yamamoto, Nature **456**, 218 (2008).
7. J. Berezovsky, M. H. Mikkelsen, N. G. Stoltz, L. A. Coldren, and D. D. Awschalom, Science **320**, 349 (2008).
8. M. T. Rakher, L. Ma, O. Slattery, X. Tang, and K. Srinivasan, Nat. Photonics **4**, 786 (2010).
9. M. T. Rakher, L. Ma, M. Davano, O. Slattery, X. Tang, and K. Srinivasan, Phys. Rev. Lett. **107**, 083602 (2011).
10. C. Langrock, E. Diamanti, R. V. Roussev, Y. Yamamoto, M. M. Fejer, and H. Takesue, Opt. Lett. **30**, 1725 (2005).
11. J. S. Pelc, L. Ma, C. R. Phillips, Q. Zhang, C. Langrock, O. Slattery, X. Tang, and M. M. Fejer, Opt. Express **19**, 21445 (2011).
12. H. Takesue, Phys. Rev. A **82**, 013833 (2010).
13. N. Curtz, R. Thew, C. Simon, N. Gisin, and H. Zbinden, Opt. Express **18**, 22099 (2010).
14. J. S. Pelc, C. Langrock, Q. Zhang, and M. M. Fejer, Opt. Lett. **35**, 2804 (2010).
15. S. Zaske, A. Lenhard, and C. Becher, Opt. Express **19**, 12825 (2011).
16. R. V. Roussev, C. Langrock, J. R. Kurz, and M. M. Fejer, Opt. Lett. **29**, 1518 (2004).
17. L. E. Myers and W. R. Bosenberg, IEEE J. Quantum Electron. **33**, 1663 (1997).
18. Q. Li, D. Marcelo, and K. Srinivasan, Nat. Photonics **10**, 406 (2016).
19. S. Zaske, A. Lenhard, C. A. Keßler, J. Kettler, C. Hepp, C. Arend, R. Albrecht, W. M. Schulz, M. Jetter, P. Michler, and C. Becher, Phys. Rev. Lett. **109**, 147404 (2012).
20. A. G. Radnaev, Y. O. Dudin, R. Zhao, H. H. Jen, S. D. Jenkins, A. Kuzmich, and T. A. B. Kennedy, Nat. Phys. **6**, 894 (2010).
21. H. Dong, H. Pan, L. Yao, E. Wu, and H. Zeng, Appl. Phys. Lett. **93**, 071101 (2008).
22. H. Kamada, M. Asobe, T. Hongo, H. Takesue, Y. Tokura, Y. Nishida, O. Tadanaga, and H. Miyazawa, Opt. Lett. **33**, 639 (2008).
23. J. S. Pelc, Q. Zhang, C. R. Philips, L. Yu, Y. Yamamoto, and M. M. Fejer, Opt. Lett. **37**, 476 (2012).
24. A. P. Vandevender and P. G. Kwiat, J. Mod. Opt. **51**, 1433 (2004).
25. M. H. Chou, J. Hauden, M. A. Arbore, and M. M. Fejer, Opt. Lett. **23**, 1004 (1998).
26. R. Regener and W. Sohler, Appl. Phys. B **36**, 143 (1985).